Adsorption of Lennard-Jones fluid mixture in a planar slit: A perturbative density functional approach

Niharendu Choudhury and Swapan K. Ghosh
Theoretical Chemistry Section, RC and CD Division, Chemistry Group, Bhabha Atomic Research Centre, Mumbai 400 085, India
(Received 17 March 2000 revised manuscript received 11 May 2001; published 27 July 2001)

A simple perturbative density functional approach is employed to investigate the adsorption behavior of a model Lennard-Jones fluid confined in a slitlike pore. Adsorption of one-component fluid as well as two-component fluid mixtures in varying pore sizes has been investigated. The results on the density profiles and the excess adsorption obtained from this theory are found to be in overall good agreement with the available computer simulation results. The results are also compared with the same from some recent weighted density based calculations.

DOI: 10.1103/PhysRevE.64.021206 PACS number(s): 61.20.Gy, 68.43.−h

I. INTRODUCTION

During the last two decades, the study of the structure of fluids and their mixtures in confined geometries [1–4] has been an interesting area of research in liquid state physics because of its relevance to various interesting phenomena [3] such as adsorption, wetting, surface driven phase transitions, separation of fluid components from their mixtures etc. As a result, there has been an upsurge of interest in the field of theoretical as well as computer simulation studies of fluids in pores, slits, and other restricted geometries [1]. Fluids confined in a particular geometry become inhomogeneous with respect to the density distribution because of the wall-fluid interaction and also the excluded volume effect. Although integral equation theory [5] for a homogeneous fluid has been extended and applied to various problems of inhomogeneous fluids, in recent times it is the density functional theory (DFT) [6,7] that has occupied the center stage in the field of inhomogeneous fluids. DFT has become an immensely popular and powerful tool for handling a many-particle system because of its inherent conceptual and computational simplicity and also wide applicability to a large class of problems in the classical [6–8] as well as the quantum domain [9,10].

In DFT, the single particle density $\rho(\mathbf{r})$ is used as the basic variable [9]. The grand potential of an inhomogeneous many-particle system is written as a functional of $\rho(\mathbf{r})$ [7], which on minimization leads to an Euler-Lagrange equation for obtaining the true equilibrium density distribution. The exact functional form of part of this energy functional is however not known in general for an inhomogeneous density distribution and hence the crux of the problem lies in finding a suitable approximation [2] for this functional. For selected systems with homogeneous density, however, this functional is often known within the framework of some approximate theories and very often this has formed the basis of arriving at approximate functional forms for corresponding systems with inhomogeneous density distributions. One of the most widely used approximations is the weighted density approximation (WDA) [2] where either the free energy or the one-particle correlation function of the inhomogeneous system is mapped into that of the corresponding homogeneous system of a suitable effective smoothed density obtained through a suitable averaging process. Some of the versions of WDAs that are extensively used in predicting the structure of an inhomogeneous fluid are due to Tarazona [11], Curtin and Ashcroft [12], Rosenfeld, Kierlik and Rosinberg [13], Denton and Ashcroft (DA) [14] to name a few and they differ from each other in the way the effective smoothed density is calculated and also how it is used to calculate the functional. The WDA based approaches are quite successful in predicting the structure of a one-component fluid near one or two walls and some of them have been extended to binary mixtures [15–17], electrolyte solutions [18], colloidal dispersions [19,20], studies of freezing [21,22], crystal-melt interfaces [23] etc. and the results obtained from these approaches are in quite good agreement with the corresponding computer simulation results [15,24,25]. Most of these weighted density based methods (except a few) that are nonperturbative in nature are however computationally demanding and in general their application to complex systems is somewhat restricted.

An alternative perturbative route based on a functional Taylor expansion in density inhomogeneity around the homogeneous density provides however the simplest approach for approximating the free energy functional of an inhomogeneous system. Although the expansion is in principle exact, due to the lack of knowledge of the higher order correlation functions appearing in this expansion, one has to enforce truncation usually at the second order [26], whereas in WDA the effects of all the higher order correlations are taken into account in an approximate manner. Failure of this truncated perturbative expansion in various problems is normally attributed to the neglect of the higher order correlations (beyond second order). In a recent interesting work, Sweatman [27] has analyzed various aspects of the truncated density expansions in a perturbative approach.

Recently, attempts have been made to retain terms upto third order in the functional Taylor series expansion. Since the third order correlation function is unknown for most of the model systems even if the density is uniform, Rickayzen and coworkers [28,29] have approximated the three-body correlation function with its parameters determined by forcing the free energy functional of the inhomogeneous fluid to reproduce the correct bulk pressure for the uniform fluid. This approach has been successfully applied to a hard sphere system [28,29] and has been extended to study various complex systems such as colloidal and other systems in planar

[30,31] and cylindrical [32] geometries restricted mainly to the one-component case. Subsequently, this perturbative approach has been extended [33,34] to the case of a binary hard sphere mixture and the results obtained for the density profiles of both the components are in good agreement with simulation as well as DA WDA approach [33]. Compared to some WDA based approaches, computational effort associated with the perturbative approach is much less and hence its application to complex systems should be easier.

The Lennard-Jones (LJ) fluid is an interesting model system to study because of the presence of the attraction term in addition to the repulsive part in the interparticle interaction potential. The structure of LJ fluid confined in a slit pore has been extensively studied using DFT based approaches [35–41] as well as through simulation [42–46]. Therefore, quite a few results are available to compare with and thereby verify the validity of the third order perturbative approach for the LJ system. The main objective of the present paper is therefore to test and assess the applicability of this perturbative approach to a more general LJ system. We have studied here the structure and adsorption behavior of a one-component LJ fluid as well as a two-component LJ fluid mixture confined in slit pores.

The remaining part of the paper is organized as follows. In Sec. II we discuss the general density functional formalism with the perturbative approximation for a two-component LJ fluid mixture while the numerical results are presented in Sec. III. Finally we offer a few concluding remarks in Sec. IV.

II. DENSITY FUNCTIONAL THEORY FOR THE INHOMOGENEOUS LJ FLUID MIXTURE

In DFT, the grand potential $\Omega[\rho_1,\rho_2]$ of a two-component fluid mixture is a unique functional of its component density distributions $\rho_1(\mathbf{r})$ and $\rho_2(\mathbf{r})$ for fixed external potentials $u_1(\mathbf{r})$ and $u_2(\mathbf{r})$ corresponding to the two components and is given by

$$\Omega[\rho_1,\rho_2]=F[\rho_1,\rho_2]+\sum_{i=1}^{2}\int d\mathbf{r}[u_i(\mathbf{r})-\mu_i]\rho_i(\mathbf{r}), \quad (1)$$

where μ_i is the chemical potential of the ith component. Here $F[\rho_1,\rho_2]$, the intrinsic Helmholtz free energy of the system, is a universal functional of the densities for a fixed interparticle potential, consisting of a noninteracting ideal free energy F_{id} representing the free energy of a noninteracting system of the same density and the excess free energy, F_{ex} arising due to interparticle interaction, i.e.,

$$F[\rho_1,\rho_2]=F_{\mathrm{id}}[\rho_1,\rho_2]+F_{\mathrm{ex}}[\rho_1,\rho_2]. \quad (2)$$

The functional form of the ideal part of the free energy F_{id} is explicitly known and for a two-component system, it is given by

$$F_{\mathrm{id}}[\rho_1,\rho_2]=\beta^{-1}\sum_{i=1}^{2}\int d\mathbf{r}\rho_i(\mathbf{r})\{\ln[\rho_i(\mathbf{r})\Lambda_i^3]-1\}, \quad (3)$$

where $\beta[=1/k_BT$, with k_B as the Boltzmann constant] is the inverse temperature and Λ_i represents the thermal de-Broglie wavelength. The grand potential functional $\Omega[\rho_1,\rho_2]$ of Eq. (1) assumes a minimum value at the true equilibrium densities and hence its minimization leads to the equation for the inhomogeneous density distributions given by

$$\rho_i(\mathbf{r})=\rho_i^0\exp\{-\beta u_i(\mathbf{r})+c_i^{(1)}(\mathbf{r};[\rho_1(\mathbf{r}),\rho_2(\mathbf{r})]) -\tilde{c}_i^{(1)}(\rho_1^0,\rho_2^0)\}, \quad (4)$$

where the chemical potential of the inhomogeneous system has been equated to that of the bulk phase of uniform bulk densities ρ_1^0 and ρ_2^0 and $-\beta^{-1}\tilde{c}_i^{(1)}(\rho_1^0,\rho_2^0)$ represents the excess chemical potential of the bulk phase of uniform bulk densities ρ_1^0 and ρ_2^0.

This key equation of DFT, although derived for obtaining the density distribution of an inhomogeneous fluid mixture, is useful to obtain information about the properties of the homogeneous fluid as well. Thus, if the external potential $u_i(\mathbf{r})$ in the above equation is replaced by the interparticle potential $\phi_{ji}(r)$ acting between the jth particle tagged at the origin and the ith particle located at a point $\mathbf{r}$, one obtains with the help of the Percus relation

$$\rho_{ji}^{\phi}(\mathbf{r})=\rho_i^0 g_{ji}(r) \quad (5)$$

a simple method to calculate the radial distribution function $g_{ji}(r)$.

The quantity $c_i^{(1)}$ in Eq. (4) denotes the one-particle direct correlation function (DCF) defined as

$$c_i^{(1)}(\mathbf{r};[\rho_1,\rho_2])=-\beta\frac{\delta F_{\mathrm{ex}}[\rho_1,\rho_2]}{\delta\rho_i(\mathbf{r})}, \quad (6)$$

and $\tilde{c}^{(1)}$ denotes the same in the bulk phase. It may be noted that the form of Eq. (4) is the same as the Boltzmann distribution for an ideal gas and all the effects of interparticle interactions enter through the DCF $c_i^{(1)}(\mathbf{r};[\rho_1,\rho_2])$ that plays the role of an effective one-particle potential in DFT. In order to solve Eq. (4) for the density distribution, one needs $c_i^{(1)}(\mathbf{r};[\rho_1,\rho_2])$ or $F_{\mathrm{ex}}[\rho_1,\rho_2]$, the exact functional forms of which are unfortunately not known for most inhomogeneous systems and hence suitable approximation for either of these two quantities is to be made.

In this work, we consider only the perturbative approach based on a functional Taylor expansion for the evaluation of $c_i^{(1)}$ of the inhomogeneous system. Thus, retaining terms upto third order in density inhomogeneity $\Delta\rho_i(\mathbf{r})=[\rho_i(\mathbf{r})-\rho_i^0]$, the quantity $c_i^{(1)}(\mathbf{r};[\rho_1,\rho_2])$ can be expressed as

$$\begin{aligned}c_i^{(1)}(\mathbf{r}_1;[\rho_1,\rho_2])=\tilde{c}_i^{(1)}([\rho_1^0,\rho_2^0])+\sum_{j=1}^{2}\int d\mathbf{r}_2 \\ \times\tilde{c}_{ij}^{(2)}(\mathbf{r}_1,\mathbf{r}_2;[\rho_1^0,\rho_2^0])\Delta\rho_j(\mathbf{r}_2) \\ +\frac{1}{2}\sum_{j=1}^{2}\sum_{k=1}^{2}\int\int d\mathbf{r}_2 d\mathbf{r}_3 \\ \times\tilde{c}_{ijk}^{(3)}(\mathbf{r}_1,\mathbf{r}_2,\mathbf{r}_3)\Delta\rho_j(\mathbf{r}_2)\Delta\rho_k(\mathbf{r}_3).\end{aligned} \quad (7)$$

The quantities $c_{ij}^{(2)}$ and $c_{ijk}^{(3)}$ denote the second and third order DCF's defined, respectively, as

$$c_{ij}^{(2)}(\mathbf{r}_1,\mathbf{r}_2) = -\beta \frac{\delta^2 F_{\rm ex}[\rho_1,\rho_2]}{\delta\rho_i(\mathbf{r}_1)\,\delta\rho_j(\mathbf{r}_2)} \tag{8}$$

and

$$c_{ijk}^{(3)}(\mathbf{r}_1,\mathbf{r}_2,\mathbf{r}_3) = -\beta \frac{\delta^3 F_{\rm ex}[\rho_1,\rho_2]}{\delta\rho_i(\mathbf{r}_1)\,\delta\rho_j(\mathbf{r}_2)\,\delta\rho_k(\mathbf{r}_3)}. \tag{9}$$

and $\tilde{c}_{ij}^{(2)}$ and $\tilde{c}_{ijk}^{(3)}$ in Eq. (7) refer to the same for the homogeneous fluid mixture, a knowledge of which is essential for implementation of the present scheme for calculation of the density profiles.

The quantity $\tilde{c}_{ij}^{(2)}$ can be obtained by numerically solving the Ornstein-Zernike (OZ) equation for the homogeneous fluid mixture, viz.,

$$h_{ij}(r_{12}) = \tilde{c}_{ij}^{(2)}(r_{12}) + \sum_{k=1}^{2} \rho_k^0 \int d\mathbf{r}_3 \tilde{c}_{ik}^{(2)}(r_{13}) h_{kj}(r_{32}) \tag{10}$$

combined with the closure

$$h_{ij}(r_{12}) + 1 = \exp[-\beta\phi_{ij}(r_{12}) + h_{ij}(r_{12}) - \tilde{c}_{ij}^{(2)}(r_{12}) + B_{ij}(r_{12})] \tag{11}$$

involving the total correlation function $h_{ij}(r_{12})[=g_{ij}(r_{12})-1]$, the interparticle potential $\phi_{ij}(r_{12})$, and the bridge function $B_{ij}(r_{12})$ that provides a measure of the interparticle correlations. For the LJ fluid mixture under consideration, an approximate $B_{ij}(r_{12}) = B(s_{ij}(r_{12}))$, which is proposed by Duh and Henderson [47] recently and used here is given by

$$B(s) = \begin{cases} \dfrac{-s^2}{2\left[1+\left(\dfrac{5s+11}{7s+9}\right)s\right]} & \text{for} \quad s \geqslant 0 \\ -\dfrac{1}{2}s^2 & \text{for} \quad s < 0 \end{cases}, \tag{12}$$

where $s \equiv s_{ij}(r_{12})$ denotes

$$s_{ij}(r_{12}) = h_{ij}(r_{12}) - \tilde{c}_{ij}^{(2)}(r_{12}) - u_{2,ij}(r_{12}) \tag{13}$$

and

$$u_{2,ij}(r_{12}) = -4\epsilon_{ij}\left(\frac{\sigma_{ij}}{r_{12}}\right)^6 \exp\left[\frac{-1}{\rho^*}\left(\frac{\sigma_{ij}}{r_{ij}}\right)^{6\rho^*}\right] \tag{14}$$

with $\rho^* = \Sigma_{k=1}^{2} \rho_k^0 \sigma_{kk}^3$ as the dimensionless bulk density parameter.

Although this integral equation based approach provides a route to obtain $\tilde{c}_{ij}^{(2)}(r)$ for the homogeneous LJ fluid and hence the contribution to $c_i^{(1)}(r)$ from the second order term (which we call Scheme A) in Eq. (7), this is purely numerical. An alternative approach that provides analytical expressions for $\tilde{c}_{ij}^{(2)}(r)$ of the LJ fluid is, however, possible. Since the LJ pair potential $\phi_{ij}(r_{ij})$ as given by

$$\phi_{ij}(r) = 4\epsilon_{ij}\left[\left(\frac{\sigma_{ij}}{r_{ij}}\right)^{12} - \left(\frac{\sigma_{ij}}{r_{ij}}\right)^{6}\right], \quad i,j = 1,2 \tag{15}$$

consists of a short ranged repulsive term and a relatively long ranged attractive component, the excess free energy $F_{\rm ex}$ for this system can also be partitioned into a short range part ($F_{\rm SR}$) and an attractive component ($F_{\rm att}$) viz.,

$$F_{\rm ex}[\rho_1,\rho_2] = F_{\rm SR}[\rho_1,\rho_2] + F_{\rm att}[\rho_1,\rho_2], \tag{16}$$

where the latter is often estimated within the mean field approximation as

$$F_{\rm att}[\rho_1,\rho_2] = \sum_{i=1}^{2}\sum_{j=1}^{2} \int\int d\mathbf{r}d\mathbf{r}'\,\rho_i(\mathbf{r})\rho_j(\mathbf{r}')\,\phi_{ij}^{\rm att}(|r-r'|). \tag{17}$$

For the short range repulsive part of the potential, one can introduce a reference hard sphere fluid with some suitable effective hard sphere diameter. Here, we have split the potential according to the Barker and Henderson prescription [8,48] at $r_{ij} = \sigma_{ij}$ such that the attractive part of the potential $\phi_{ij}^{\rm att}$ is represented as

$$\phi_{ij}^{\rm att}(r_{ij}) = \begin{cases} \phi_{ij}(r_{ij}), & r_{ij} > \sigma_{ij} \\ 0, & r_{ij} < \sigma_{ij} \end{cases}. \tag{18}$$

In analogy to the one-component case [49], Tan, van Swol, and Gubbins [50] have suggested an analytical expression given by

$$d_i = \frac{\alpha_1 T_i^* + \alpha_2}{\alpha_3 T_i^* + \alpha_4}, \quad i = 1,2 \tag{19}$$

for the calculation of the temperature-dependent effective hard sphere diameters d_i of the components of the LJ fluid mixture, where $T_i^*(=k_BT/\epsilon_{ii})$ is the dimensionless temperature and α_i's are constants. Here, we employ the same expression with the values of α_1, α_2, α_3, and α_4 chosen [39,51] as 0.3837, 1.0320, 0.4293, and 1.0, respectively.

This splitting of $F_{\rm ex}$ according to Eq. (16) corresponds to the mean spherical approximation of the DCF $\tilde{c}_{ij}^{(2)}$ as $\tilde{c}_{ij}^{(2)\rm SR} + \tilde{c}_{ij}^{(2)\rm LR}$, with $\tilde{c}_{ij}^{(2)\rm LR} = -\beta\phi_{ij}^{\rm att}(r_{ij})$ and $\tilde{c}_{ij}^{(2)\rm SR}$ obtainable from the $\tilde{c}_{ij}^{(2)}$ of a hard sphere fluid mixture of effective diameters d_1 and d_2 of the two components. We call this method of obtaining $\tilde{c}_{ij}^{(2)}$ and hence the contribution of the second order term in Eq. (7), Scheme B.

Although the two-particle DCF $\tilde{c}_{ij}^{(2)}$ can thus be obtained rather accurately for the homogeneous fluid by either of the two schemes, $\tilde{c}_{ijk}^{(3)}$ is however completely unknown and hence an approximation for this quantity is essential. Following the original work of Rickayzen and co-workers [29], an approximation for $\tilde{c}_{ijk}^{(3)}$ as obtained recently [33,34] can be written as

$$\tilde{c}^{(3)}_{ijk}(\mathbf{r}_1,\mathbf{r}_2,\mathbf{r}_3)=\int d\mathbf{r}_4 L_i(\mathbf{r}_4,\mathbf{r}_1)L_j(\mathbf{r}_4,\mathbf{r}_2)L_k(\mathbf{r}_4,\mathbf{r}_3),$$

$$i,j,k=1,2, \tag{20}$$

where L_1 and L_2 are the two two-body functions for components 1 and 2, respectively, and are given by

$$L_i(|\mathbf{r}-\mathbf{r}'|)=B_i a_i(|\mathbf{r}-\mathbf{r}'|), \quad i=1,2 \tag{21}$$

consisting of a density dependent constant B_i and a size-dependent function $a_i(r)$ satisfying the normalization $\int a_i(\mathbf{r})d\mathbf{r}=1$. The model $a_i(r)$ that has been assumed by us [33] is given by the step function form

$$a_i(r)=\frac{6}{\pi d_i^3}\Theta\left(\frac{d_i}{2}-r\right). \tag{22}$$

The two constants B_1 and B_2 can be determined from the requirement that the density functional as used here should yield the correct bulk pressure in the homogeneous limit. In this work, we have assumed, for simplicity, these two constants to be equal, i.e., $B_1=B_2$ and B_1 is then obtained from the equation

$$\beta P=-\beta\Omega_0[\rho_1^0,\rho_2^0]/V=\sum_{i=1}^{2}\rho_i^0-\frac{1}{2}\sum_{i=1}^{2}\sum_{j=1}^{2}\rho_i^0\rho_j^0\int d\mathbf{r}_2$$
$$\times\tilde{c}^{(2)}_{ij}(\mathbf{r}_1,\mathbf{r}_2;[\rho_1^0,\rho_2^0])+\frac{B_1^3}{6}\left(\sum_{i=1}^{2}\rho_i^0\right)^3. \tag{23}$$

A more rigorous derivation of Eq. (23) has been given by Sweatman [27] who has clearly delineated the role of involving zero density fluid as well as the bulk fluid as the reference. Alternative prescriptions for $a_i(r)$ and evaluation of B_i have also been given by Rickayzen and co-workers [34].

Thus, we have two schemes for the calculation of the density distribution. The final form for the density equation in Scheme A is given by

$$\rho_i(\mathbf{r})=\rho_i^0\exp\Bigg\{-\beta u_i(\mathbf{r})+\sum_{j=1}^{2}\int d\mathbf{r}_2\tilde{c}^{(2)}_{ij}(\mathbf{r},\mathbf{r}_2;[\rho_1^0,\rho_2^0])$$
$$\times\Delta\rho_j(\mathbf{r}_2)+\frac{1}{2}B_i\int d\mathbf{r}_2 a_i(\mathbf{r},\mathbf{r}_2)\left(\sum_{j=1}^{2}B_j\overline{\delta\rho_{jj}(r_2)}\right)^2\Bigg\} \tag{24}$$

with the quantity $\overline{\delta\rho_{jk}(\mathbf{r}_2)}$ defined as

$$\overline{\delta\rho_{jk}(\mathbf{r}_2)}=\int d\mathbf{r}_3 a_j(\mathbf{r}_2,\mathbf{r}_3)\Delta\rho_k(\mathbf{r}_3) \tag{25}$$

and is to be solved after obtaining $\tilde{c}^{(2)}_{ij}$ by solving Eqs. (10)–(14) using the bulk densities ρ_1^0 and ρ_2^0 only once in the beginning.

The final form for the density equation in Scheme B is given by

$$\rho_i(\mathbf{r})=\rho_i^0\exp\Bigg\{-\beta u_i(\mathbf{r})+\sum_{j=1}^{2}\int d\mathbf{r}_2\overline{c^{(2)\mathrm{SR}}_{ij}}(\mathbf{r},\mathbf{r}_2;[\rho_1^0,\rho_2^0])$$
$$\times\Delta\rho_j(\mathbf{r}_2)+\frac{1}{2}B_i\int d\mathbf{r}_2 a_i(\mathbf{r},\mathbf{r}_2)\left(\sum_{j=1}^{2}B_j\overline{\delta\rho_{jj}(\mathbf{r}_2)}\right)^2$$
$$-\beta\sum_{i=1}^{2}\int d\mathbf{r}_2\Phi^{\mathrm{att}}_{ij}(|\mathbf{r}-\mathbf{r}_2|)\Delta\rho_j(\mathbf{r}_2)\Bigg\}. \tag{26}$$

Thus, in this scheme we essentially have a two-component mixture of a reference hard sphere fluid with bulk densities ρ_1^0 and ρ_2^0 and hard sphere diameters d_1 and d_2 for the two components, respectively. The homogeneous mixture is characterized by the diameter ratio $\alpha(=d_1/d_2)$, the concentration $x=\rho_2^0/\rho_0$ with $\rho_0=\rho_1^0+\rho_2^0$, and the bulk packing fraction η defined as

$$\eta=\frac{\pi}{6}[\rho_1^0 d_1^3+\rho_2^0 d_2^3]=\frac{\pi}{6}[x+(1-x)\alpha^3]\rho_0 d_2^0. \tag{27}$$

Here we follow the convention $d_1<d_2$ and the ratio $\alpha<1$.

The two-particle DCF $\tilde{c}^{(2)(\mathrm{SR})}_{ij}(r_{12})$ for the hard sphere mixture in bulk phase is known approximately from Lebowitz's solution [52] of the PY integral equation as

$$-c^{(2)\mathrm{SR}}_{ii}(r)=a_i+b_i r+d r^3, \quad r<d_i, \quad i=1,2$$
$$-c^{(2)\mathrm{SR}}_{12}(r)=\begin{cases} a_i, & r\leqslant\lambda \\ a_1+[by^2+4\lambda dy^3+dy^4]/r, & \lambda\leqslant r\leqslant d_{12} \\ 0, & r>d_{12}, \end{cases} \tag{28}$$

where $\lambda=(d_2-d_1)/2$, $d_{12}=(d_1+d_2)/2$ and $y=r-\lambda$. The coefficients a_i, b_i, b, and d are given by simple but lengthy expressions of η, α, and x as have been given elsewhere [52]. The bulk pressure for the hard sphere mixture has also been obtained by Lebowitz [52] and is given by

$$\frac{\beta P}{\rho_0}=\frac{(1+\xi_3+\xi_3^2)}{(1-\xi_3)^3}-3\eta_1 x\left(\frac{1}{\alpha}-1\right)^2\Bigg[\left(1+\frac{1}{\alpha}\right)$$
$$+d_2\xi_2\Bigg]\Big/(1-\xi_3)^3 \tag{29}$$

where $\eta_1=(\pi/6)\rho_1^0 d_1^3$ and $\xi_n=(\pi/6)\Sigma_{i=1}^{2}\rho_i^0 d_i^n$. This expression corresponds to the compressibility pressure, while the most widely used expression of pressure for a one-component hard sphere fluid is the Carnahan-Starling expression given by

$$\frac{\beta P}{\rho_0}=\frac{1+\eta+\eta^2-\eta^3}{(1-\eta)^3} \tag{30}$$

in terms of the packing fraction η. These two expressions for the bulk pressure alongwith $\tilde{c}^{(2)(\mathrm{SR})}_{ij}(r)$ given by Eq. (28) have been used here in Eq. (23) for the evaluation of the constant B_1.

The inhomogeneous fluids that we consider here consist of a one-component LJ fluid as well as a two-component LJ fluid mixture confined in slit pores made up of two smooth parallel graphite walls of infinite area, separated by a distance H. Due to planar geometry of the system, the density variation is only in the z direction perpendicular to the wall (xy plane) and hence the evaluation of $\rho_i(z)$ can be simplified by analytically carrying out the integrals over the x and y coordinates. The external potential $u_i(z)$ in this case is the sum of the contributions from the two walls located at $z=0$ and $z=H$ respectively, i.e.,

$$u_i(z)=\phi_{\rm sf}(z)+\phi_{\rm sf}(H-z), \tag{31}$$

where z is the distance of the fluid particle from the first wall and $\phi_{\rm sf}$ is the solid-fluid model potential, the exact form of which is discussed later. Besides the density distribution, the other important quantities of interest are the excess adsorption per unit area, which is defined as

$$\Gamma_i=\int_0^H [\rho_i(z)-\rho_i^0]dz \tag{32}$$

from which the mean pore density can be calculated as

$$\rho_{p_i}=\frac{\Gamma_i}{H}+\rho_i^0 \tag{33}$$

for each component $i=1,2$. The total excess adsorption for the mixture is obtained as

$$\Gamma=\Gamma_1+\Gamma_2. \tag{34}$$

III. RESULTS AND DISCUSSION

Equations (24) and (26) for the density profiles are nonlinear integral equations that have been solved by using a self-consistent iterative procedure with $\rho_i(z)=\rho_i^0$ as the initial guess. Due to planar symmetry of the problem, these equations have been reduced to one-dimensional forms by analytically integrating over the other two directions. The remaining one-dimensional integrals have been evaluated numerically using the trapezoidal rule and by means of a simple discretization scheme with a uniform mesh. The convergence criterion used for the iterative procedure has been such that the average mean square density deviation between successive iterations is very small. The distance from the wall and the densities of the two components have been made dimensionless in terms of σ_{11} such that z and ρ_i can be expressed as $z^*=z/\sigma_{11}$ and $\rho_i^*=\rho_i\sigma_{11}^3$, respectively, and temperature, pressure, and chemical potential have been measured in dimensionless forms as $T^*=k_BT/\epsilon_{11}$, $P^*=P\sigma_{11}^3/\epsilon_{11}$, and $\mu^*=\mu/\epsilon_{11}$. The other quantities such as Γ_i, ρ_p, and Γ are also expressed in terms of the dimensionless quantities $\Gamma_i^*=\Gamma_i\sigma_{11}^2$, $\Gamma^*=\Sigma_{i=1}^2\Gamma_i^*$ and $\rho_{p_i}^*=\rho_{p_i}\sigma_{11}^3$, respectively. Throughout this work we have not used any cutoff for the attractive potential.

To test the validity and applicability of the theoretical approach used here for the study of adsorption of LJ fluid in a slit pore, we have first calculated $g(r)$ of a one-component LJ fluid at $T^*=1.5$ and $\rho_0^*=0.7$. The results from the present approach are shown alongwith the simulation results [53] in Fig. 1 and the agreement is found to be quite good. This establishes the predictability of the method for density distribution around a test particle.

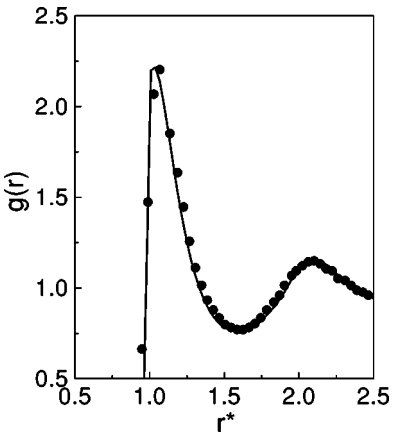

FIG. 1. Plot of radial distribution function $g(r)$ vs $r^*(=r/\sigma)$ for a pure Lennard-Jones fluid of bulk density $\rho_0^*=0.7$ at $T^*=1.50$. The results from Scheme B of the present theory are shown by solid lines and simulation results (from Ref. [53]) are shown as circles.

A. Adsorption of pure LJ fluid

We present here results on the density profile and excess adsorption as obtained from this perturbative theory for various one-component inhomogeneous LJ fluids, for which the interaction potential between a fluid particle and the carbon atom on the graphite wall is modeled by the Lennard-Jones 10-4-3 potential [54] given by

$$\phi_{\rm sf}(z)=2\pi\epsilon_{\rm sf}\rho_s\sigma_{\rm sf}^2\Delta\left[\frac{2}{5}\left(\frac{\sigma_{\rm sf}}{z}\right)^{10}-\left(\frac{\sigma_{\rm sf}}{z}\right)^4-\frac{\sigma_{\rm sf}^4}{3\Delta(0.61\Delta+z)^3}\right] \tag{35}$$

where ρ_s and Δ characterize the solid wall surface and $\sigma_{\rm sf}$ and $\epsilon_{\rm sf}$ are the parameters for the wall-fluid potential. The wall-fluid parameters $\sigma_{\rm sf}$ and $\epsilon_{\rm sf}$ are obtained through the Lorentz-Berthelot mixing rules, using the values of $\sigma_{\rm ss}$, $\epsilon_{\rm ss}$ for the solid and $\sigma_{\rm ff}$, $\epsilon_{\rm ff}$ for the fluid, viz., $\epsilon_{\rm sf}=(\epsilon_{\rm ss}\epsilon_{\rm ff})^{1/2}$ and $\sigma_{\rm sf}=(\sigma_{\rm ss}+\sigma_{\rm ff})/2$.

We first consider the case of a LJ system for which systematic simulation studies have been reported [44,45]. In this case, the solid atoms on the wall are chosen to be identical to the particle in the fluid, i.e., $\sigma_{\rm ss}=\sigma_{\rm ff}=\sigma_{\rm sf}$, $\epsilon_{\rm ss}=\epsilon_{\rm ff}=\epsilon_{\rm sf}$ and the values of Δ and $\rho_s\sigma_{\rm sf}^2\Delta$ are taken as $1/\sqrt{2}\sigma_{\rm ff}$ and 1.0, respectively. The other parameters characterizing the fluid are the reduced temperature $T^*=1.2$ and reduced chemical potential $\mu^*=-2.477$ that fixes [44] the bulk density $\rho_0^*=0.5925$ and bulk pressure $P^*=0.24$. The density profiles from our theory (Scheme B) for $H^*=H/\sigma_{11}=3,4$ and 7.5 with the bulk density $\rho_0^*=0.5925$ are presented in Figs. 2–4 along with the corresponding computer simulation and Kier-

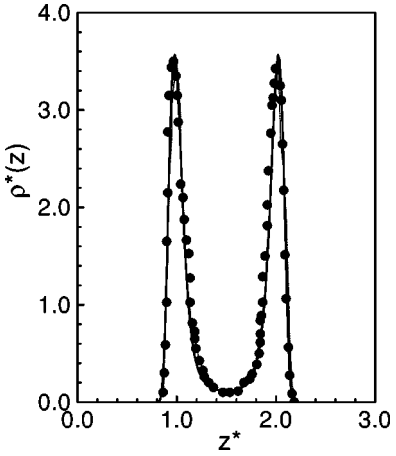

FIG. 2. Plot of density profiles $\rho^*(z)$ vs z^* for a pure Lennard-Jones fluid of bulk density $\rho_0^*=0.5925$ in a planar slit of width $H^*=3$ at $T^*=1.20$. The results from Scheme B of the present theory are shown by solid lines, results from Kierlik-Rosinberg WDA are shown by dotted lines and simulation results (from Ref. [45]) are shown as circles.

lik and Rosinberg (KR) WDA [39(a)] results. The overall agreement between the results from our theory (Scheme B), KR WDA and simulation is quite satisfactory. In Fig. 5, we have plotted the results on the density profile of ethylene confined in a carbon slit pore of width $H^*=5$ at temperature $T^*=1.35$ where ethylene is modeled as LJ fluid with the parameters chosen as $\sigma_{11}=0.4218\,\mathrm{nm}$, $\epsilon_{11}/k_B=201.8\,\mathrm{K}$ and the wall-fluid parameters as $\sigma_{sf}=0.3809\,\mathrm{nm}$ ($\sigma_s=0.340\,\mathrm{nm}$), $2\pi\rho_s\epsilon_{sf}\sigma_{sf}^2\Delta=12.96\epsilon_{11}$, and $\Delta=0.3393\,\mathrm{nm}$. The bulk density ρ_0^* for this system corresponding to the chemical potential $\mu^*=\mu/\epsilon_{11}=-3$ is 0.28. Grand canonical Monte Carlo (GCMC) simulation on this system has been carried out by van Megan and Snook [42], Walton and Quirke [43], and recently by Tan and Gubbins [35]. Calculated results from DFT based on WDA are also available [36,39]. The density profile for this system is compared with

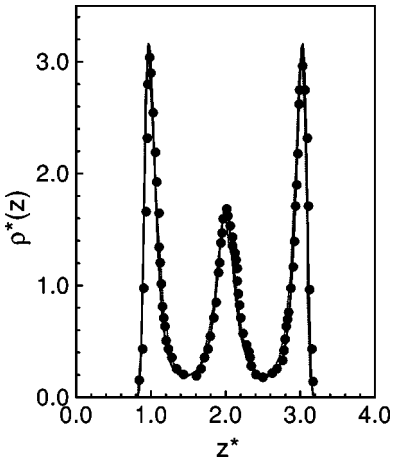

FIG. 3. Plot of density profiles $\rho^*(z)$ vs z^* for a pure Lennard-Jones fluid of bulk density $\rho_0^*=0.5925$ in a planar slit of width $H^*=4$ at $T^*=1.20$. The key is the same as in Fig. 2. Simulation results are taken from Ref. [45].

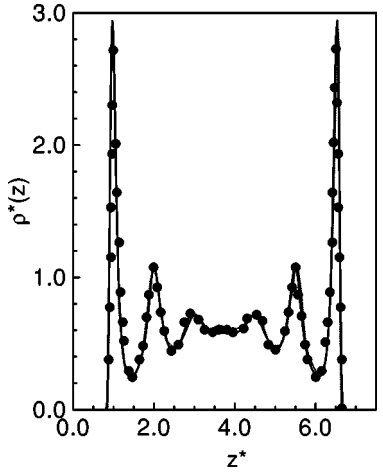

FIG. 4. Plot of density profiles $\rho^*(z)$ vs z^* for a pure Lennard-Jones fluid of bulk density $\rho_0^*=0.5925$ in a planar slit of of width $H^*=7.5$ at $T^*=1.20$. The key is the same as in Fig. 2. Simulation results are taken from Ref. [44].

KR WDA [39(a)] and the simulation results [39,43] in this figure and it is observed that the present result is in overall good agreement although the second peak from the wall is somewhat underpredicted by our theory. In the inset of this figure, we have compared the density profiles obtained from Scheme B of the present approach with the same calculated by using an interparticle potential cutoff at $r_c=2.5\sigma$ and the results are found not to differ significantly from each other. It may be noted that the simulation results used for comparison correspond to the use of cutoff at $r_c^*=2.5$. The mean pore density as obtained from our theory is $\rho_p^*=0.546$ and the corresponding simulation result is 0.564. The results for the excess adsorption Γ^* as defined by Eq. (32) as a function of ρ_0^* for the same system has been plotted in Fig. 6 alongwith the KR WDA [39(a)] and simulation results [35(a), 39(a)] of

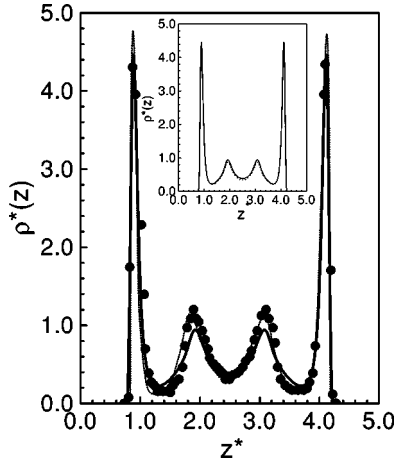

FIG. 5. Plot of density profiles $\rho^*(z)$ vs z^* for ethylene of bulk density $\rho_0^*=0.28$ in a carbon slit of width $H^*=5$ at $T^*=1.35$. The key is the same as in Fig. 2. Simulation results are taken from Ref. [43] (also reproduced in Ref. [39(a)]). In the inset results from Scheme B of the present theory with a cutoff ($r_c=2.5\sigma$) shown by solid lines are compared with the same without cutoff ($r_c=\infty$).

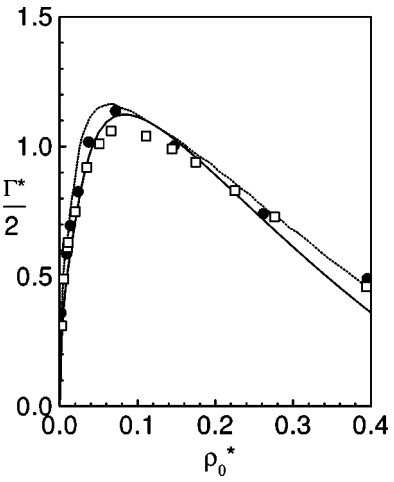

FIG. 6. Plot of excess adsorption isotherm per unit area Γ^* vs ρ_0^* of ethylene in carbon slit pore of width $H^*=5$ at $T^*=1.35$. The key is the same as in Fig. 2. Simulation results that are shown as circles are taken from Ref. [35(a)] (also reproduced in Ref. [39(a)]) and those shown as open squares are taken from Ref. [41].

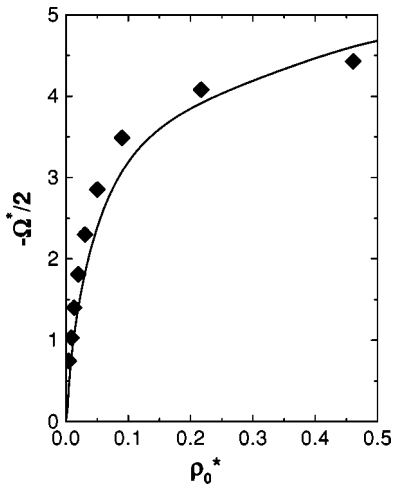

FIG. 7. Plot of excess grand potential $\Omega^*(=\Omega^{ex}\sigma^2/A\epsilon)$ vs ρ_0^* corresponding to the same system as in Fig. 6. The results from the Scheme B of the present theory are shown by solid lines and simulation results (from Ref. [41]) are shown as solid squares.

Tan and Gubbins as well as of Sweatman [41]. The excess adsorption curve passes through a maximum that is characteristic of the adsorption of fluid at supercritical temperatures. The overall agreement between the present theory and simulation is good, although the excess adsorption at higher density is slightly underpredicted by our theory. It may be noted that the excess adsorption is also related to the excess (over bulk) grand potential Ω^{ex} through the Gibbs adsorption equation given by

$$\Gamma = -\left(\frac{\partial \Omega^{ex}}{\partial \mu}\right)_{T,A} \tag{36}$$

In order to obtain Ω^{ex}, we have numerically integrated this equation with respect to the chemical potential μ using Γ corresponding to Fig. 6. The calculated results are shown in Fig. 7 alongwith the recently reported [41] simulation data and a reasonably good agreement is observed.

B. Adsorption of binary LJ fluid mixture

We also consider the implementation of our theory for the case of a binary LJ mixture confined in a planar slit. The external potential due to wall-fluid interaction for the ith component in the mixture $\phi_{sf} \equiv \phi_{si}$ is modeled by the (9, 3) LJ potential, which also represents a graphite wall and is given by

$$\phi_{si}(z) = \frac{3\sqrt{3}}{2}\epsilon_{si}\left[\left(\frac{\sigma_{si}}{z}\right)^9 - \left(\frac{\sigma_{si}}{z}\right)^3\right], \quad i=1,2, \tag{37}$$

where quantities with subscript si are the wall-fluid parameters for the i th component. There are a few simulation studies for the structure of a LJ mixture in a slit pore. Here we consider the argon-krypton mixture modeled as a LJ fluid mixture for which the parameters are: $\sigma_{11}=0.3405$ nm, $\sigma_{22}=0.3630$ nm, $\epsilon_{11}/k_B=109.8$ K, and $\epsilon_{22}/k_B=163.1$ K with the cross parameters calculated by using Lorentz-Berthelot mixing rule. Argon is taken as the smaller component denoted by $i=1$ whereas krypton corresponds to $i=2$. This system has been studied by Sokolowski and Fischer [38] using molecular dynamics (MD) simulation as well as the DFT based approach of Meister-Kroll-Groot and later by Kierlik and Rosinberg [39] with their version of WDA [13]. The solid-fluid potential parameters are the same as those used in earlier studies [38,39], i.e., $\sigma_{s1}/\sigma_1=0.5621$, $\sigma_{s2}/\sigma_1=0.588$, $\epsilon_{s1}/\epsilon_{11}=9.2367$, and $\epsilon_{s2}/\epsilon_{11}=12.1744$. Density profiles for the two components that we present here in Fig. 8 are calculated at supercritical temperature $T^*=k_BT/\epsilon_{11}=2$ and at a total bulk density $\rho_0^*=0.444$, and mole

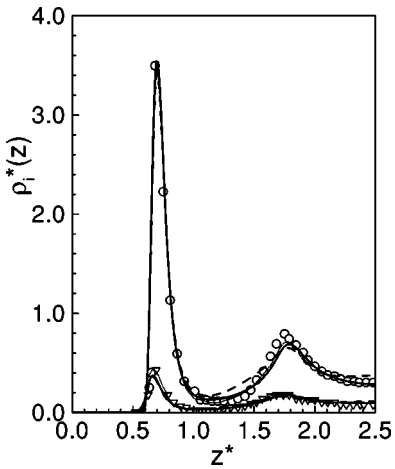

FIG. 8. Plot of density profiles $\rho_i^*(z)$ vs z^* for an argon-krypton fluid mixture confined in graphite slit pore of width $H^*=5$ at $T^*=2.0$. The total bulk density and mole fraction of krypton are $\rho_0^*=0.444$ and $x=0.738$, respectively. Dashed lines correspond to results from Scheme A of the present approach, solid lines are from Scheme B of the present approach, dotted lines correspond to KR WDA results. Simulation results (from Ref. [38]) for krypton are shown by open circles and results for argon by open triangles.

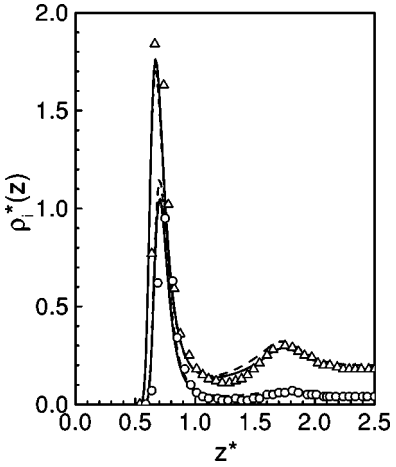

FIG. 9. Plot of density profiles $\rho_i^*(z)$ vs z^* for an argon-krypton fluid mixture confined in graphite slit pore of width $H^*=5$ at $T^*=2.0$. The total bulk density and mole fraction of krypton are $\rho_0^*=0.103$ and $x=0.109$, respectively. Dashed lines and solid lines are from the calculation using Scheme A and Scheme B of the present theory respectively. Simulation results (from Ref. [38]) for krypton are shown by open circles and results for argon by open triangles.

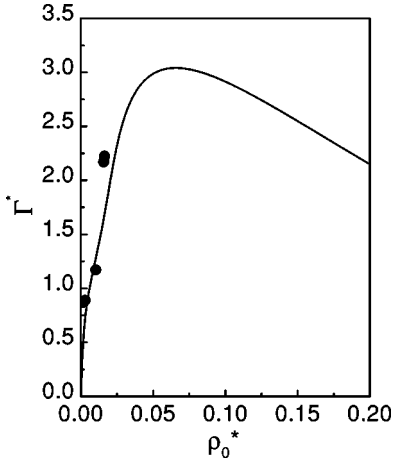

FIG. 10. Plot of total excess adsorption Γ^* obtained from Scheme B of the present theory as a function of the total bulk density ρ_0^* for the argon-krypton fluid mixture with mole fraction of krypton $x=0.333$ confined in a graphite slit pore of width $H^*=5$ at $T^*=1.5$. The key is the same as in Fig. 1. Simulation results are taken from Ref. [38].

fraction of krypton $x=0.738$ for a slit width $H^*=5$. The present results from both Scheme A and B are found to compare quite well with those obtained from the MD simulation of Sokolowski and Fischer [38] as well as with KR WDA [39(a)] that have also been included in this figure. Since both the Schemes A and B lead to comparable results, it appears that, that the partitioning scheme in this case yields a DCF, which is similar to the numerically calculated one based on the OZ equation and hence it is easier to pursue the simple Scheme B. It may be noted that we have plotted the results only for half the slit. We obtain the excess adsorptions for Ar, $\Gamma_1^*=-0.158$ and for Kr, $\Gamma_2^*=0.48$ that are to be compared with the MD simulation results $\Gamma_1^*=-0.14$ and $\Gamma_2^*=0.51$. In Fig. 9, we plot the calculated density profiles from both Scheme A and B for the same system with total bulk density $\rho_0^*=0.103$ and $x=0.109$ alongwith the corresponding computer simulation results [38] for comparison. Finally in Fig. 10, we present the result for the total excess adsorption isotherm as defined by Eqs. (32) and (34) as a function of the total density ρ_0^* at a reduced temperature $T^*=1.5$ and mole fraction of krypton $x=0.333$ alongwith a few points from the computer simulation result of Sokolowski and Fischer [38]. The excess adsorption is found to pass through a maximum at an intermediate density.

IV. CONCLUDING REMARKS

We have presented here a simple density functional investigation of the adsorption behavior of a LJ fluid mixture within the framework of a perturbative approximation for the free energy functional and hence the first order DCF of the binary hard sphere mixture. The predictions of the density profiles as well as the excess adsorption from the theory presented here are almost of the same accuracy as that of KR WDA that is an established weighted density functional theory and bears a comparable computational effort. It is also worthwhile to mention that in an interesting recent analysis, Sweatman [27] has shown that density functionals with truncated density expansion are thermodynamically inconsistent as they do not satisfy the Gibbs adsorption equation. This is a consequence of the fact that the excess free energy F_{ex} corresponding to Eq. (7) that employs a truncated version of the exact functional Taylor expansion with an infinite number of terms in general may depend on the bulk density ρ_0 around which the expansion is carried out. The full infinite series expansion although explicitly contains ρ_0 is however independent of ρ_0 since the expression is an exact one. Therefore, there must be cancellation effect of this dependence as higher order terms are retained. Since comparison of our results with results obtained from KR WDA (which satisfies Gibbs adsorption equation) and from simulation show overall good agreement, the bulk density dependence of our F_{ex} may be negligible at least for the systems investigated in the present study. This is also evident from the reasonably good agreement of the calculated results on excess grand potential with simulation [41]. However, for system parameters for which adsorption is high, F_{ex} as calculated here might be bulk density dependent [27] and hence performance of the present theory can be tested for various other systems at different physical parameters to gain further insight. Recently, other versions [55,56] of perturbative DFT based approaches have also been developed for the study of nonuniform LJ fluids. Application of the present method to other systems with long range interaction such as the Yukawa mixture or electrolyte solution etc. will be interesting to investigate and studies in these directions are in progress. Further extension of this theory to other kind of geometries (e.g., cylindrical and spherical) are also in progress.

ACKNOWLEDGMENTS

It is pleasure to thank Dr. T. Mukherjee and Dr. J. P. Mittal for their kind interest and encouragement.

[1] For a review, see *Fundamentals of Inhomogeneous Fluids*, edited by D. Henderson (Marcel Dekker, New York, 1992).

[2] For a review, see R. Evans, in *Fundamentals of Inhomogeneous Fluids*, edited by D. Henderson (Marcel Dekker, New York, 1992).

[3] D. E. Sullivan and M. M. Telo da Gama, in *Fluid Interfacial Phenomena*, edited by C. A. Croxton (Wiley, New York, 1986).

[4] S. Dietrich, in *Phase Transition and Critical Phenomena*, edited by C. Domb and J. L. Lebowitz (Academic, New York, 1988).

[5] For a review, see D. Henderson, in *Fundamentals of Inhomogeneous Fluids*, edited by D. Henderson (Marcel Dekker, New York, 1992).

[6] P. Hohenberg and W. Kohn, Phys. Rev. **136**, B864 (1964); N. D. Mermin, Phys. Rev. **137**, A1441 (1965); W. F. Saam and C. Ebner, Phys. Rev. A **15**, 2566 (1977).

[7] R. Evans, Adv. Phys. **28**, 143 (1979).

[8] J. P. Hansen and I. R. McDonald, *Theory of Simple Liquids*, 2nd ed. (Academic, London, 1986).

[9] For a review, see S. K. Ghosh and B. M. Deb, Phys. Rep. **92**, 1 (1982); in *Single Particle Density in Physics and Chemistry*, edited by N. H. March and B. M. Deb (Academic, New York, 1987).

[10] R. G. Parr and W. Yang, *Density Functional Theory of Atoms and Molecules* (Oxford University Press, New York, 1989).

[11] P. Tarazona, Mol. Phys. **52**, 81 (1984); Phys. Rev. A **31**, 2672 (1985).

[12] W. A. Curtin and N. W. Ashcroft, Phys. Rev. A **32**, 2909 (1985); Phys. Rev. Lett. **56**, 2775 (1986).

[13] Y. Rosenfeld, Phys. Rev. Lett. **63**, 980 (1989); E. Kierlik and M. L. Rosinberg, Phys. Rev. A **42**, 3382 (1990).

[14] A. R. Denton and N. W. Ashcroft, Phys. Rev. A **39**, 426 (1989).

[15] Z. Tan, U. M. B. Marconi, F. van Swol, and K. E. Gubbins, J. Chem. Phys. **90**, 3704 (1989).

[16] A. R. Denton and N. W. Ashcroft, Phys. Rev. A **42**, 7312 (1990).

[17] A. R. Denton and N. W. Ashcroft, Phys. Rev. A **44**, 8242 (1991).

[18] C. N. Patra and S. K. Ghosh, J. Chem. Phys. **102**, 2556 (1994); Phys. Rev. E **49**, 2826 (1994).

[19] N. Choudhury and S. K. Ghosh, J. Chem. Phys. **104**, 9563 (1996).

[20] N. Choudhury and S. K. Ghosh, Phys. Rev. E **53**, 3847 (1996).

[21] A. R. Denton and N. W. Ashcroft, Phys. Rev. A **39**, 4701 (1989).

[22] N. Choudhury and S. K. Ghosh, Phys. Rev. E **51**, 4503 (1995), and references therein.

[23] W. A. Curtin, Phys. Rev. Lett. **59**, 1228 (1987); Phys. Rev. B **39**, 6775 (1989); D. W. Marr and A. P. Gast, Phys. Rev. E **47**, 1212 (1993); R. Ohnesorge, H. Lowen, and L. Wagner, *ibid.* **50**, 4801 (1994); N. Choudhury and S. K. Ghosh, *ibid.* **57**, 1939 (1998).

[24] I. K. Snook and D. Henderson, J. Chem. Phys. **68**, 2134 (1978).

[25] R. L. Davidchack and B. B. Laird, Phys. Rev. E **54**, R5905 (1996); J. Chem. Phys. **108**, 9452 (1998).

[26] T. V. Ramakrishnan and M. Yussouff, Phys. Rev. B **19**, 2775 (1979); For a review, see Y. Singh, Phys. Rep. **207**, 351 (1991); A. D. J. Haymet and D. W. Oxtoby, J. Chem. Phys. **74**, 2559 (1981); A. D. J. Haymet, Annu. Rev. Phys. Chem. **38**, 89 (1987).

[27] M. B. Sweatman, Mol. Phys. **98**, 573 (2000).

[28] G. Rickayzen and A. Augousti, Mol. Phys. **52**, 1355 (1984).

[29] M. Calleja, A. N. North, J. G. Powles, and G. Rickayzen, Mol. Phys. **73**, 973 (1991).

[30] N. Choudhury and S. K. Ghosh, J. Chem. Phys. **108**, 7493 (1998).

[31] T. H. Yoon and S. C. Kim, Phys. Rev. E **58**, 4541 (1998); S. C. Kim and S. H. Suh, *ibid.* **56**, 2889 (1997); J. H. Yi and S. C. Kim, J. Chem. Phys. **107**, 8147 (1997).

[32] N. Choudhury and S. K. Ghosh, J. Chem. Phys. **111**, 1737 (1999).

[33] N. Choudhury and S. K. Ghosh, J. Chem. Phys. **110**, 8628 (1999).

[34] M. Moradi and G. Rickayzen, Mol. Phys. **66**, 143 (1989).

[35] (a) Z. Tan and K. E. Gubbins, J. Phys. Chem. **94**, 6061 (1990); in *Characterization of Porous Solids II*, edited by International Union of Pure and Applied Chemistry (Elsevier, Amsterdam, 1991); (b) P. B. Balbuena, D. Berry, and K. E. Gubbins, J. Phys. Chem. **97**, 937 (1993); P. B. Balbuena and K. E. Gubbins, Langmuir **9**, 1801 (1993); C. Lastoskie, K. E. Gubbins, and N. Quirke, J. Phys. Chem. **97**, 4786 (1993); C. Lastoskie, K. E. Gubbins, and N. Quirke, Langmuir **9**, 2693 (1993).

[36] J. G. Powles, G. Rickayzen, and M. L. Williams, Mol. Phys. **64**, 33 (1988).

[37] Z. Tan, K. E. Gubbins, F. van Swol, and U. M. B. Marconi, in *Proceedings of the Third International Conference on Fundamental Adsorption, Sonthofen*, edited by A. B. Mersmann and S. E. Scholl (Engineering Foundation, New York, 1991); G. S. Heffelfinger, Z. Tan, K. E. Gubbins, U. M. B. Marconi, and F. van Swol, Mol. Simul. **2**, 393 (1989); S. Jiang and K. E. Gubbins, J. Phys. Chem. **98**, 2403 (1994); S. L. Sowers and K. E. Gubbins, Langmuir **11**, 4758 (1994); Z. Tan and K. E. Gubbins, J. Phys. Chem. **96**, 845 (1992); Z. Tan and K. E. Gubbins, *ibid.* **98**, 2403 (1994).

[38] S. Sokolowski and J. Fischer, Mol. Phys. **71**, 393 (1990).

[39] (a) E. Kierlik and M. L. Rosinberg, Phys. Rev. A **44**, 5025 (1991); (b) E. Kierlik, M. L. Rosinberg, J. E. Finn, and P. A. Monson, Mol. Phys. **75**, 1435 (1992).

[40] S. K. Bhatia, Langmuir **14**, 6231 (1998).

[41] M. B. Sweatman, Phys. Rev. E **63**, 031102 (2001).

[42] W. van Megan and I. K. Snook, Mol. Phys. **54**, 741 (1985).

[43] J. P. R. B. Walton and N. Quirke, Chem. Phys. Lett. **129**, 382 (1986).

[44] I. K. Snook and W. van Megan, J. Chem. Phys. **72**, 2907 (1980); **74**, 1409 (1981).

[45] J. J. Magda, M. Tirell, and H. T. Davis, J. Chem. Phys. **83**, 1888 (1985).

[46] K. G. Ayappa, Langmuir **14**, 880 (1998).

[47] D.-M. Duh and D. Henderson, J. Chem. Phys. **104**, 6742 (1996).

[48] J. Barker and D. Henderson, J. Chem. Phys. **47**, 7414 (1967).

[49] B. Q. Lu, R. Evans, and M. M. Telo da Gama, Mol. Phys. **55**, 1319 (1985).

[50] Z. Tan, F. van Swol, and K. E. Gubbins, Mol. Phys. **62**, 1213 (1987).

[51] L. Verlet and J. J. Weis, Phys. Rev. A **5**, 939 (1972).
[52] J. L. Lebowitz, Phys. Rev. **133**, 895 (1964).
[53] D. Duh, D. Henderson, L. Mier-Y-Teran, and S. Sokolowski, Mol. Phys. **90**, 563 (1997).
[54] W. A. Steele, Surf. Sci. **36**, 317 (1973).
[55] S. Zhou and E. Ruckenstein, J. Chem. Phys. **112**, 5242 (2000).
[56] N. Choudhury and S. K. Ghosh, J. Chem. Phys. **114**, 8530 (2001).